Plasma angular momentum effects and twisted incoherent scatter radar beams

T. B. Leyser,[1] F. Waldemarsson,[1,2] and S. C. Buchert[1]

Received 11 July 2011; revised 19 June 2012; accepted 30 July 2012; published 14 September 2012.

[1] Phased arrays provide new possibilities for remote sensing with radars. By imposing an azimuthal phase variation, electromagnetic beams that carry orbital angular momentum can be formed. Such beams have a phase structure that appears twisted and as a result an intensity null in the center of the beam cross section. Here we numerically investigate twisted beams for incoherent scatter radars that are used to study the ionosphere. We discuss the possibility of utilizing such radar beams to probe twisted beams of plasma waves and flows transverse to the beam axis, such as associated with auroral arcs. Transverse plasma flows may give rise to a rotational frequency shift of the scatter from a twisted beam and Doppler broadening due to the beam divergence, the latter also occurring with regular beams. Although the angular momentum effects of the considered large scale flows are generally small, sheared and vortical flows transverse to the beam axis can in principle be discriminated from unidirectional flows with beams carrying orbital angular momentum.

Citation: Leyser, T. B., F. Waldemarsson, and S. C. Buchert (2012), Plasma angular momentum effects and twisted incoherent scatter radar beams, *Radio Sci.*, *47*, RS5004, doi:10.1029/2011RS004819.

1. Introduction

[2] An electromagnetic field can carry angular momentum as polarization, orbital angular momentum (OAM) and a mixture thereof. Spin (polarization) is an intrinsic property of photons i.e., photons always come with spin. Photons may in addition carry OAM. On the classical level OAM arises as a result of the spatial distribution of the phase of the electromagnetic field and is typically carried by certain configurations of beams, particularly beams with helical, twisted, phase fronts.

[3] OAM of laser light was identified in the early 1990s in paraxial beams with a Laguerre–Gaussian field amplitude distribution [*Allen et al.*, 1992]. The exploration of twisted light and twisted photons has since become a field of active research [*Molina-Terriza et al.*, 2007].

[4] Electromagnetic fields that carry OAM have also been investigated in the radio frequency domain. Theoretical estimates showed that the ponderomotive force exerted by a radio beam in a plasma has a specific contribution from the OAM of the field [*Istomin*, 2002]. Numerical simulations demonstrated that it is possible to form twisted beams with a circular phased array of a limited number of antenna elements [*Thidé et al.*, 2007]. Methods for determining the OAM modes at radio frequencies by single-point measurements or by measuring one electric field component in two points have been suggested [*Mohammadi et al.*, 2010a, 2010b]. The first experiments transmitting twisted radio beams to the ionosphere were conducted at the High Frequency Active Auroral Research Program (HAARP) in Alaska, USA [*Leyser et al.*, 2009]. It has further been predicted theoretically that groups of ion acoustic waves (phonons) and Langmuir waves (plasmons) too may carry OAM and be excited by stimulated Brillouin and Raman scattering with twisted beams [*Mendonça et al.*, 2009b].

[5] Phased arrays provide new possibilities for remote sensing with radars. By imposing an azimuthal phase variation in the currents in the antenna elements around the array, beams with helical phase fronts can be transmitted. The phase pattern of such beams appears twisted. The azimuthal phase variation is associated with an effective azimuthal wave vector component, in addition to the usual wave vector determined by the radar frequency and direction of the beam. Twisted radar beams can thus be used to detect angular momentum effects and azimuthal plasma flows transverse to the radar beam. To detect OAM the azimuthal phase variation in the received scattered beam must be measured, for example, by comparing the phases of the currents in the spatially distributed receiving antenna elements in the phased array.

[6] Here we discuss applications of twisted beams for incoherent scatter radars used for ionospheric studies. In a plasma in thermal equilibrium the fluctuations in the electron and ion concentrations are statistically independent. A radar pulse scattered from such a plasma gives rise to standard incoherent scatter spectra, with its so-called ion line from the ion acoustic fluctuations and plasma lines from the Langmuir fluctuations. However, spatial correlations between the fluctuations may be introduced by plasma flows and electrostatic waves.

[1]Swedish Institute of Space Physics, Uppsala, Sweden.
[2]Now at Westinghouse Electric Sweden AB, Västerås, Sweden.

Corresponding author: T. B. Leyser, Swedish Institute of Space Physics, Box 537, SE-751 21 Uppsala, Sweden. (thomas.leyser@irfu.se)

0048-6604/12/2011RS004819

[7] *Knudsen et al.* [1993] investigated plasma flows along auroral arcs and transverse to the geomagnetic field in a bistatic radar geometry, using the UHF system of the European Incoherent Scatter facilities (EISCAT). Here the plasma motion had a component along the beam, but was varying rapidly in time and/or over spatial scales less than the beam width, which resulted in an apparent widening of the ion line spectrum. In typical active auroras the widening can be substantial and would unaccounted lead to overestimation of the ion temperature. A large number of measurements are along the geomagnetic field, and, thus, are not affected in the way described by *Knudsen et al.* [1993]. However, in the following we will note two ways in which even geomagnetic field-aligned measurements are affected by rapidly varying, small scale field-perpendicular motion.

[8] Even a regular monostatic beam with a nonzero divergence makes the radar sensitive to plasma flows transverse to the beam axis. In subvolumes within the beam and off its center the scattering wave vector has a component transverse to the beam axis and pointing everywhere toward the center. A uniform flow across the beam will Doppler shift the spectrum from each subvolume and apparently widen the observed spectrum which is integrated over the beam cross section. This effect has, to our knowledge, not been considered in studies of the ion and electron temperatures and, for example, Joule heating.

[9] Rotating and spiraling structures in magnetized plasma are receiving increasing attention. For example, optical aurora has been studied for a long time and may exhibit both larger scale spirals, vortex streets and small-scale curls. Fine structure of the aurora has been reviewed by *Sandahl et al.* [2008]. However, the heating by the associated small-scale electric fields remains an issue in theories, simulations and measurements [*Cosgrove and Codrescu*, 2009]. In the present treatment we investigate the effects of spatial correlations on the incoherent scatter spectra, specifically the effect of sheared and vortical plasma flows that occur within the beam and transverse to the beam axis. The angular momentum effects of the considered large scale plasma flows on incoherent scatter spectra are found to be small and rather high degrees of twisting of narrow beams are required, which puts challenging conditions on the array antenna used. However, the requirements on the radar for detecting electrostatic plasma vortices appear less stringent.

2. Electromagnetic OAM

[10] The electromagnetic angular momentum **J** can be expressed in terms of the electromagnetic linear momentum density $\mathbf{p} = \varepsilon_0 \mathbf{E} \times \mathbf{B}$, where **E** is the electric field and **B** is the magnetic field:

$$\mathbf{J} = \int \mathbf{r} \times \mathbf{p}\, d^3 r \tag{1}$$

where the integration is over all space. With $\mathbf{B} = \nabla \times \mathbf{A}$ we can write for vacuum [*Jackson*, 1999]

$$\mathbf{J} = \varepsilon_0 \int \mathbf{E} \times \mathbf{A}\, d^3 r + \varepsilon_0 \int \sum_{n=1}^{3} E_n (\mathbf{r} \times \nabla) A_n d^3 r \equiv \mathbf{S} + \mathbf{L} \tag{2}$$

where **S** can be referred to as the spin (polarization) angular momentum and **L** the OAM.

[11] The most well known twisted electromagnetic beam is the paraxial Laguerre-Gaussian beam. The fields for this type of beam include the azimuthal phase factor $\exp(il\varphi)$ in addition to a cylindrically symmetric amplitude distribution, where φ is the azimuthal angle and l is an integer. At a given time, the phase of the field thus varies by $l2\pi$ for a full turn around the beam axis in a plane transverse to that axis. Laguerre-Gaussian beams have well-defined OAM proportional to l [*Allen et al.*, 1992]. For $l \neq 0$ there is an intensity null on the beam axis, where the azimuthal phase is ambiguous.

[12] An example of a non-paraxial beam is the Bessel beam, which has field amplitudes proportional to $\exp(il\varphi)$ $J_l(ka \sin \phi)$, where J_l is the l:th order Bessel function of the first kind, $k = |\mathbf{k}|$ is the vacuum wave number, a is the radius of the circular antenna array, and ϕ is the angle between **k** and the beam axis. Whereas to generate a true non-diffractive Bessel beam requires infinite energy, an approximate Bessel beam can be generated by a circular array of dipole antennas [*Knudsen*, 1953; *Mohammadi et al.*, 2010a]. Such a beam too has an OAM proportional to l [*Mohammadi et al.*, 2010a].

[13] The azimuthal phase variation $\exp(il\varphi)$ implies that the field has helical phase fronts and that there are $|l|$ helices intertwined, which is why we refer to such a field as twisted. This spatial variation of the phase in the plane transverse to the beam axis can be associated with an effective azimuthal wave vector. For an azimuthal phase $\Phi = l\varphi$, the azimuthal wave vector components are [*Gori et al.*, 1998]

$$k_x = \frac{\partial \Phi}{\partial x} = -l \frac{\sin\varphi}{\rho}, \quad k_y = \frac{\partial \Phi}{\partial y} = l \frac{\cos\varphi}{\rho}, \tag{3}$$

where $\varphi = \arctan(y/x)$ and $\rho = (x^2 + y^2)^{1/2}$. The z-axis is along the beam axis. These effective wave vector components are distinct from the usual wave vector of a plane electromagnetic wave that is determined by the phase velocity and frequency. The effective azimuthal wave vector depends on the spatial variation of the phase of the electromagnetic field, that is, the interference pattern of the plane waves that can be considered to compose the beam. Thus, if one had an antenna that some how mimicked the ring-shaped power distribution of a twisted beam but without the azimuthal phase variation, such a beam would not have azimuthal wave vector components as in equation (3) and not carry OAM; momentum is associated with spatial variation of phase.

[14] To transmit a beam that carries OAM one must impose the azimuthal phase variation $\exp(il\varphi)$ on the currents of the antenna elements around the phased array, transverse to the beam axis. For comparison, if all antenna currents have the same phase ($l = 0$) a regular beam is transmitted. To measure OAM in a received beam one must in a reciprocal way detect the phase $\exp(il\varphi)$ in the currents of the spatially distributed receiving antenna elements of the array.

3. Model

[15] To investigate effects of large scale plasma flow on incoherent scatter radar measurements we compute an ideal

incoherent scatter spectrum which is then shifted in frequency, due to Doppler and/or rotational frequency shift, both of which are explained below. The incoherent scatter spectrum is computed by following *Hagfors* [1961], for the case of an unmagnetized and non-collisional plasma in thermal equilibrium. The approximation of an unmagnetized plasma for the ionosphere is applicable to radar frequencies much higher than the electron plasma frequency and viewing angles close to the geomagnetic field direction (nearly antiparallel in the northern hemisphere).

[16] The plasma dispersion function is computed by the numerical method of *Weideman* [1994]. Regarding computational speed and control over numerical precision, this method seems to have advantages over older ones, for example those based on *Fried and Conte* [1961]. We have tested that our code using the Weideman method gives results consistent with the method of Fried and Conte [*Swartz*, 1978].

[17] Flows in the plasma may Doppler shift the frequency spectrum of the incoherent scatter. The nonrelativistic translational Doppler shift is given by

$$\Delta\omega_{\mathrm{D}} = \mathbf{k}\cdot\mathbf{v}, \tag{4}$$

where in our case $\mathbf{v}$ is the plasma flow velocity and $\mathbf{k}$ is the wave vector of the scattering ion acoustic fluctuations; $\mathbf{k}$ is determined by the radar frequency and scattering geometry:

$$\mathbf{k} = \mathbf{k}_{\mathrm{r}} - \mathbf{k}_{\mathrm{t}}, \tag{5}$$

where $\mathbf{k}_{\mathrm{r}}$ ($\mathbf{k}_{\mathrm{t}}$) is the wave vector of the received (transmitted) electromagnetic wave. Here we consider a monostatic radar so that with a radar frequency much larger than the frequency of ion acoustic waves, $\mathbf{k}_{\mathrm{r}} \approx -\mathbf{k}_{\mathrm{t}}$ and $\mathbf{k} \approx -2\mathbf{k}_{\mathrm{t}}$. Thus, the wavelength probed by the radar is approximately half that of the radar, the latter being approximately equal to the vacuum wavelength for typical radar frequencies of the order of one hundred megahertz and higher.

[18] In addition to the usual Doppler shift there can occur a nonrelativistic rotational frequency shift given by [*Courtial et al.*, 1998]

$$\Delta\omega_{\mathrm{R}} = j\Omega, \tag{6}$$

where $j = l + s$ is the total angular momentum number of the radar beam ($s = \pm 1$ is the spin) and Ω is the angular velocity between the radar and scattering medium. Contrary to the Doppler shift, $\Delta\omega_{\mathrm{R}}$ is independent of the radar frequency. Further, whereas $\Delta\omega_{\mathrm{D}}$ depends on $\mathbf{v}$ having a component along the radar wave vector, $\Delta\omega_{\mathrm{R}}$ arises from motion transverse to the radar beam axis.

[19] It is illustrative to consider the Doppler shift from a rotational flow for a twisted beam with azimuthal wave vector components given by equation (3). The rotational axis of the flow is aligned with the beam axis. Starting with equation (4) for the Doppler shift and with a velocity field $v_x = -\Omega\rho\sin\varphi$, $v_y = -\Omega\rho\cos\varphi$, we can write:

$$\begin{aligned}\Delta\omega_{\mathrm{D}} &= k_x v_x + k_y v_y \\ &= -l\frac{\sin\varphi}{\rho}(-\Omega\rho\sin\varphi) + l\frac{\cos\varphi}{\rho}\Omega\rho\cos\varphi \\ &= l\Omega,\end{aligned} \tag{7}$$

where we recognize the rotational frequency shift given by equation (6). The rotational frequency shift can thus in this case be interpreted as a Doppler shift resulting from the wave vector components that are transverse to the beam axis and associated with the OAM of the beam.

[20] From equation (6) we see that a circularly polarized beam ($s = \pm 1$) too gives rise to a rotational frequency shift, although there is no OAM in the beam ($l = 0$). This frequency shift can be derived from conservation of energy and angular momentum considerations [*Garetz*, 1981]. A way of visualizing the rotational frequency shift is to consider a circularly polarized field for which the electric field rotates with the frequency ω. An observer rotating with the frequency Ω will observe an electric field at the shifted frequency $\omega \pm \Omega$, depending on the sense of rotation.

[21] The ionospheric scatter is modeled by several thousand evenly spaced points in a cross section of the beam, at a range of 200 km along the geomagnetic field in the F region, where the ions follow the plasma convection. At each point the plasma flow velocity is specified and the Doppler shift according to equation (4) is computed. The rotational frequency shift given by equation (6) is the same in each point; for a regular beam it has a contribution from the circular polarization of the field and for a twisted beam both from the polarization and OAM. These frequency shifts then give the shifted incoherent scatter spectrum. Since the radar beam intensity, I, is not constant throughout the beam cross section the spectrum amplitude is weighted by a Gaussian for a normal beam

$$I \propto \exp\left(-\frac{2\rho^2}{w^2}\right), \tag{8}$$

where cylindrical coordinates (ρ, ϕ, z) are used. For a twisted beam with its ring-shaped cross section, a Laguerre-Gaussian function (with lowest order radial index $p = 0$) is used,

$$I \propto \left(\frac{\sqrt{2}\rho}{w}\right)^{|l|}\exp\left(-\frac{2\rho^2}{w^2}\right). \tag{9}$$

The weighted spectra are then averaged to give the resulting spectrum.

[22] In the following we take the radar frequency to be 450 MHz and for a Gaussian beam use an opening angle $\theta = 1.2^\circ$ as for the Poker Flat Incoherent Scatter Radar (PFISR) in Alaska, USA. For beams carrying OAM we choose a hypothetical beam with $\theta = 1.0^\circ$. It should be noted that a phased array that gives a Gaussian beam with $\theta = 1.2^\circ$ would give a significantly wider twisted beam. The electron concentration of the plasma is taken to be $N = 5 \times 10^{11}$ m^{-3}, the electron and ion temperature $T_{\mathrm{e}} = T_{\mathrm{i}} = 1000$ K, and O^+ ions, as typical of the ionospheric F region.

4. Computational Results

[23] The effects of transverse plasma flows on the incoherent scatter spectrum are generally small. Under sunlit conditions near the F-region peak the error of the ion temperature obtained by incoherent scatter fitting software is typically 10–20 K. For a 450-MHz radar a temperature increase by 10 K would correspond to a widening of the ion line spectrum by about 0.1 kHz. Below we thus present

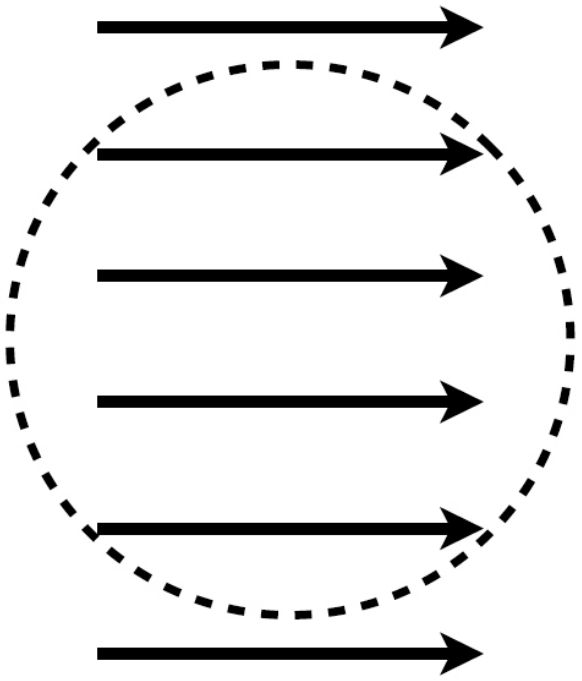

Figure 1. Schematic illustration of plasma flow transverse to the radar beam axis. The dashed circle indicates the FWHM of a Gaussian beam.

results for the required flow velocities and other parameters to obtain spectral changes of that order, unless otherwise stated.

4.1. Gaussian Radar Beams

[24] Plasma motion transverse to the radar wave vector does not give rise to a Doppler shift, as seen from equation (4). However, typical radar beams have significant divergences and thus can be viewed as a superposition of plane waves with a range of wave vectors centered around the beam axis. Therefore, a wave vector in the beam generally has a nonzero component transverse to the beam axis, which, however, for a narrow beam is much smaller than that along the axis. This implies that the scatter will be affected by plasma motion transverse to the beam. For a Gaussian beam there will be wave vector components both parallel and antiparallel to a given flow direction so that the Doppler shift will broaden the fluctuation spectrum detected by the radar.

[25] Figure 1 illustrates schematically a unidirectional plasma flow transverse to a Gaussian radar beam. The dashed circle indicates the full width at half maximum (FWHM) of the beam. Figure 2 shows two spectra of ion acoustic fluctuations, or ion lines, for a plasma drift v_x = 1.0 km/s in the x-direction transverse to the radar line-of-sight and a beam with a Gaussian intensity profile (Figure 1). For typical F-region conditions this velocity is of the order of the ion-acoustic velocity, which determines the overall width of the incoherent scatter spectrum. The dashed spectrum is for the central single transmitted wave vector that is determined by the radar frequency and radar line-of-sight. As the plasma motion occurs transverse to the radar wave vector the ion line spectrum is unaffected by the flow. The solid-line spectrum in Figure 2 is for a transmitted Gaussian beam with a FWHM of 1.2° and is slightly weaker than the dashed spectrum. In this case the radar wave vector generally has components both parallel and antiparallel to the plasma motion, depending on where in the beam, which causes a Doppler broadening of the ion line integrated over the beam cross section. For the narrow beam considered here, the slight spectral broadening implies that the ion line peaks appear about 14 Hz closer to the radar frequency whereas the base of the spectrum is slightly widened.

[26] A broader beam and/or a higher flow velocity would increase the Doppler broadening. The EISCAT UHF and EISCAT Svalbard antenna dishes produce beams with divergences of 0.5° and 0.6°, respectively, so that the spectral broadening would be roughly only half of that at PFISR. On the other hand, flows with higher Mach numbers M have been observed on occasions, higher than $M \approx 10$ (electric fields up to 600 mV/m) [*Lanchester et al.*, 1998]. If the effect is not taken into account in the data analysis (as has been the case so far, to our knowledge), the ion temperature gets overestimated accordingly.

[27] A twisted beam with a FWHM approximately that of the Gaussian beam used for Figure 2 would give approximately the same broadening of the ion line spectrum as the Gaussian beam, in the case of unidirectional transverse flow (Figure 1).

4.2. Twisted Radar Beams

[28] As seen from equation (4), plasma flow strictly transverse to the radar wave vector does not cause a Doppler shift of a backscattered signal. However, according to equation (6) a rotational frequency shift ($\Delta\omega_R$) may occur if the plasma has an angular velocity ($\Omega \neq 0$) relative to the radar and the radar beam carries angular momentum ($j \neq 0$).

[29] Figure 3 illustrates schematically the special case of a rotating plasma flow with the rotational axis coincident with the radar beam axis. The dashed circles indicate the FWHM

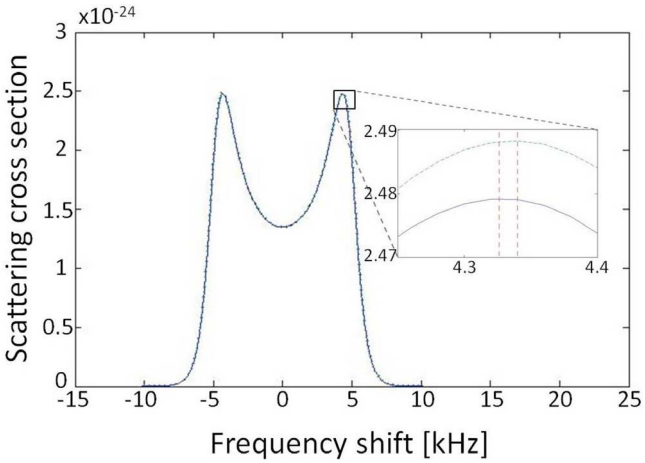

Figure 2. Ion line spectra for a plasma flow of v_x = 1 km/s transverse to the radar beam axis as illustrated in Figure 1. The frequency axis shows the shift from the radar frequency. The stronger dashed spectrum for a single radar wave vector is unaffected by the flow whereas the weaker solid-line spectrum from a Gaussian beam with a FWHM of 1.2° is slightly broadened.

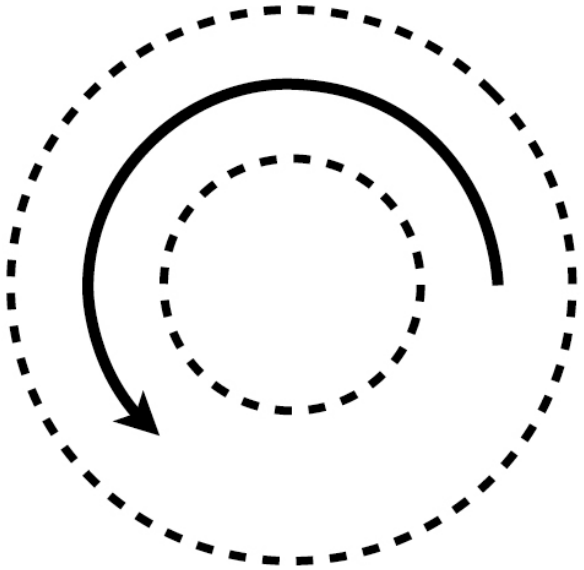

Figure 3. Schematic illustration of rotational plasma flow transverse to the radar beam axis. The dashed circles indicate the FWHM of a ring-shaped Laguerre–Gaussian beam.

of a ring-shaped Laguerre–Gaussian beam. Figure 4 shows two ion line spectra computed for the rotating plasma flow in Figure 3. As in Figure 2, the dashed spectrum is for a single transmitted radar wave vector. Since in this case the electromagnetic field does not carry angular momentum the frequency spectrum is not shifted by the rotating plasma. Further, since the flow velocity is everywhere perpendicular to the scattering wave vector the Doppler shift is zero. The solid-line spectrum is for a transmitted twisted Laguerre–Gaussian beam and exhibits a rotational frequency shift of $\Delta f_R = \Delta\omega_R/2\pi = 0.1$ kHz. As seen from equation (6), $\Delta\omega_R$ is determined by both Ω and $j = s + l$. For example, such a shift can be obtained for a twisted beam with $l = 10$, circular polarization with $s = 1$ and a plasma rotation of $\Omega = 57$ s^{-1}. This vortical plasma motion corresponds to an azimuthal speed of $v_\phi = 5.7$ km/s at $\rho = 0.1$ km and $v_\phi = 57$ km/s at $\rho = 1.0$ km. Increasing the angular momentum of the beam (larger $|l|$) increases the rotational frequency shift; alternatively, smaller angular velocities in the plasma can be detected for a given frequency resolution. We emphasize that the rotational frequency shift in Figure 4 is a result of the interaction of the transmitted beam carrying OAM and the plasma flow. OAM need not be detected in the received scattered radiation.

[30] It should be noted that strictly speaking even a linearly polarized Gaussian radar beam will result in a slightly broadened frequency spectrum since the beam consists of equal numbers of photons with opposite spin $s = \pm 1$, that is, the beam can be considered a superposition of two beams with opposite circular polarization. And according to equation (6) the spectrum will be upshifted for $s = 1$ and downshifted for $s = -1$, even though $l = 0$. For $\Omega = 57$ s^{-1}, we obtain $\Delta f_R = \pm 9$ Hz, which was neglected for the dashed spectrum in Figure 4.

[31] We also consider a more moderate plasma rotation with $\Omega = 2$ s^{-1} for which the azimuthal plasma speed at $\rho = 0.5$ km is $v_\phi = 1$ km/s. According to equation (6), for the lowest nonzero beam angular momentum ($l = 0$ and $s = 1$, for example, a circularly polarized Gaussian beam) we obtain a minute rotational frequency shift of the ion line of $\Delta f_R = 0.3$ Hz.

[32] It may be mentioned that whereas in the present treatment we only consider large scale plasma flows of the order of the radar beam diameter or larger it may be speculated that small scale vortices exist which many together filling the radar beam cross section could result in larger frequency shifts than what is discussed here. Smaller vortices may rotate faster and therefore give larger rotational frequency shifts when scattering a radar beam.

[33] Twisted beams can be used to detect sheared plasma flows transverse to the beam direction, such as associated with auroral arcs [*Haerendel et al.*, 1996]. Auroral arcs have been seen to be associated with sheared flows sometimes as large as 8 km/s [*Lanchester et al.*, 1998]. Optical measurements [*Maggs and Davis*, 1968; *Borovsky et al.*, 1991] suggest that the spatial scales of such flows could become as small as 0.1 km, the width of narrow arcs. The beam width of a typical incoherent scatter radar is a few kilometers in the F region. Thus, sheared velocity fields could well be present within such radar beams.

[34] We consider an arc in the xz-plane that is just passing the radar beam axis which we take to be parallel to the geomagnetic field and in the z-direction, the beam axis being in the plane of the shear. The flow speed in the x-direction is v_x for $y > 0$ and $-v_x$ for $y < 0$, as schematically illustrated in Figure 5. The dashed circles indicate the FWHM of a ring-shaped Laguerre–Gaussian beam. To obtain a rotational frequency shift of $\Delta f_R = 0.1$ kHz, a OAM beam mode with $l = 10$ ($s = 1$) and beam width of 1.0° requires a sheared drift

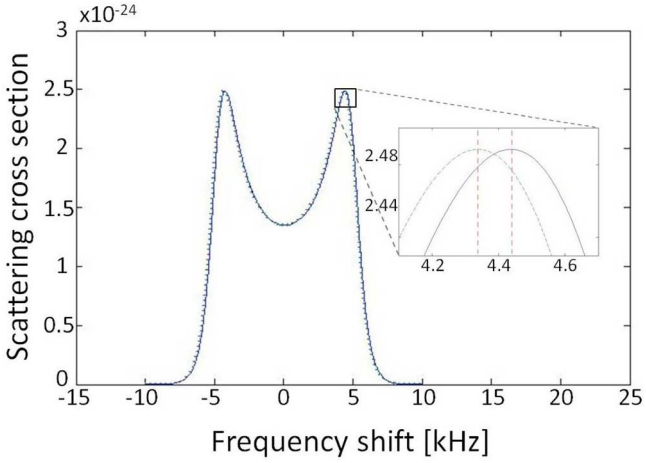

Figure 4. Ion line spectra for a rotating plasma flow with $\Omega = 57$ s^{-1} aligned with the radar beam axis as illustrated in Figure 3. The dashed spectrum for a transmitted single radar wave vector along the line-of-sight is unaffected by the flow whereas the solid-line spectrum for a transmitted Laguerre–Gaussian beam with $l = 10$, $s = 1$ and a FWHM of 1.0° is upshifted by $\Delta f_R = 0.1$ kHz.

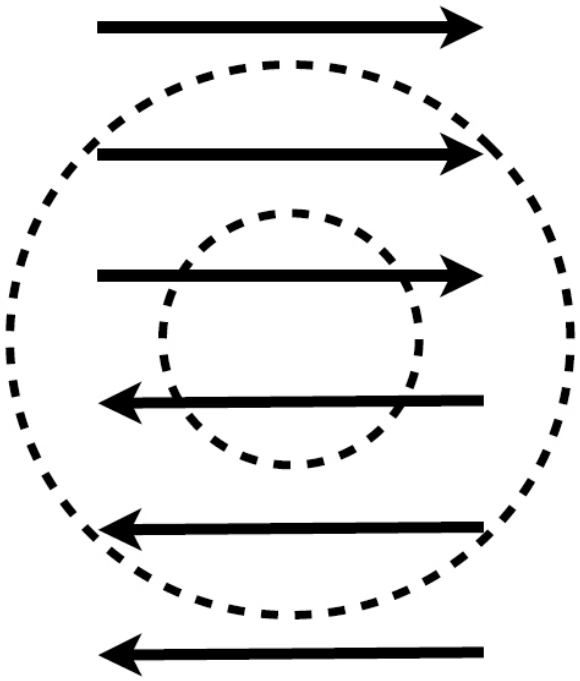

Figure 5. Schematic illustration of sheared plasma flow transverse to the radar beam axis. The dashed circles indicate the FWHM of a ring-shaped Laguerre–Gaussian beam.

speed with $v_x \approx 22$ km/s. It may be noted that with a Gaussian beam a sheared flow cannot be discriminated from a unidirectional flow transverse the radar line-of-sight (Figure 2).

[35] As seen from equation (3), a more narrow twisted beam is associated with larger effective wave vector components in the azimuthal direction ($k_{x,y} \propto 1/\rho$). Thus, a more narrow beam shows a larger frequency shift for the same drift speed. For a given frequency resolution, more narrow beams can therefore be used to detect smaller speeds. This is in contrast to the case of a rotational plasma flow aligned with the radar beam axis (Figure 4) for which there is no dependence on the radar beam opening angle.

[36] For a rotational flow with the axis of rotation aligned with the radar beam axis the flow velocity is everywhere transverse to the radar wave vector, so that the Doppler shift is zero. However, this is not the case when the plasma flow is sheared (Figure 5). In fact, for typical ionospheric parameter values, the transverse wave vector components due to a nonzero beam opening angle give a broadening of the scattered spectrum that exceeds the rotational frequency shift, in addition to a significant change in the spectral shape. Figure 6 displays the effect of the beam opening angle on the ion line spectrum (solid line) for a transmitted twisted beam scattering off the sheared plasma flow described above. The twisted beam has $\theta = 1.0°$, $l = 10$ and $s = 1$. For comparison, when effects of the beam opening angle are neglected the spectrum is only slightly distorted and shifted by the rotational frequency shift of 0.1 kHz (dashed spectrum), as a result of the azimuthal wave vector components in equation (3) associated with the angular momentum content of the transmitted beam interacting with the plasma flow. A Gaussian beam would give rise to a similar ion line as the solid-line spectrum in Figure 6, but without the effects in the dashed spectrum.

[37] Langmuir and ion acoustic wave packets may themselves occur as electrostatic beams that carry OAM [*Mendonça et al.*, 2009a, 2009b]. The waves in such beams are grouped so as to exhibit the azimuthal phase variation characteristic of OAM content discussed above. For electrostatic twisted beams the OAM constitutes the total angular momentum, in contrast to the electromagnetic case for which the angular momentum has contributions from the polarization too. It has been predicted that a Langmuir (plasmon) vortex or ion acoustic (phonon) vortex can be excited and its OAM controlled by two oppositely propagating twisted electromagnetic beams in stimulated Raman or Brillouin scattering [*Mendonça et al.*, 2009b].

[38] Twisted electrostatic beams in the plasma can be detected by twisted radar beams. We expect that naturally excited Langmuir or ion acoustic vortices would be composed of a distribution of OAM modes with different l. Plasma beams with a certain mode number $l = l_p$ could be selected by a suitable combination of transmitted and received radar OAM modes. With twisted beams there is in addition to the usual matching conditions on the frequencies and wave vectors, a condition also for the OAM mode number, as discussed by *Mendonça et al.* [2009b] for the case of nonlinear stimulation of twisted electrostatic modes:

$$l_t = l_r + l_p \tag{10}$$

where l_t, l_r, and l_p are the OAM mode numbers for the transmitted, received and plasma beam, respectively.

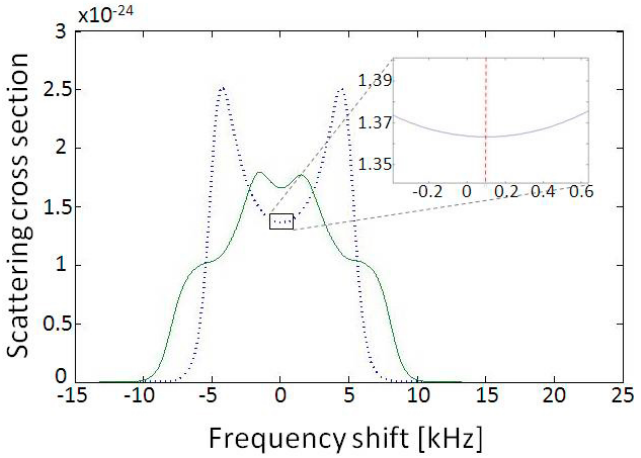

Figure 6. Ion line spectra for a transmitted Laguerre–Gaussian beam ($\theta = 1.0°$, $l = 10$ and $s = 1$) scattering off a sheared plasma flow transverse to the radar beam axis with $v_x = \pm 22$ km/s as illustrated in Figure 5. The solid-line spectrum is broadened and distorted by Doppler shifts due to the transverse wave vector components associated with the nonzero beam opening angle and upshifted by $\Delta f_R \approx 0.1$ kHz due to the radar beam twist. For comparison, we display a hypothetical ion line spectrum (dashed) that is upshifted and slightly distorted as a result of the angular momentum content in the beam, that is, Doppler effects due to the beam opening angle were artificially suppressed.

Particularly, if $l_r \neq l_t$ the coherent backscatter has occurred from a plasma vortex with $l_p \neq 0$.

[39] Whereas the rotational frequency shifts expected for radar scatter from the considered large scale plasma flows are small, as seen above, the coherent scatter from twisted ion acoustic and Langmuir beams occurs at the usual ion and plasma line frequencies, however, only at the appropriate combination of transmitted and received twisted radar beam modes, l_t and l_r.

5. Conclusions

[40] Phased arrays provide new means for remote sensing. By imposing an azimuthal phase variation such arrays can be used to transmit radar beams as well as to detect radiation carrying OAM that enable angular momentum effects to be probed, in addition to the linear momentum interaction that is commonly utilized in radar.

[41] Beams carrying OAM appear twisted with helical phase fronts. Because of phase ambiguity there is an intensity null in the center of the beam cross section. The beam twist is associated with an effective azimuthal wave vector which depends on the azimuthal phase in the beam cross section. A higher OAM mode number l and narrower beam both give a larger effective azimuthal wave vector, which is independent of the radar frequency that determines the usual wave vector.

[42] We have presented a first investigation of how to utilize the OAM dimension with incoherent scatter radars. Particularly, we propose that twisted beams can be used for the detection of plasma flows transverse to the radar beam axis as well as of twisted electrostatic beams of plasma waves, such as ion acoustic and Langmuir waves. Twisted beams can be used to discriminate sheared and vortical plasma flows from unidirectional flows transverse to the radar beam axis. Whereas here we have been concerned with incoherent scatter radars, twisted beams are relevant to any radar and remote sensing applications for detection of angular momentum effects.

[43] However, the effects of the considered large scale plasma flows transverse to the radar beam axis on the incoherent scatter spectrum are generally expected to be small for conditions in the auroral ionosphere, even for rather high OAM mode numbers l and narrow beams. Thus, apart from discussing the use of OAM in radar in principle, our results indicate the level of measurement precision and beam forming capability that may be needed to detect the rotational frequency shift in future ionospheric radar systems. It must be emphasized that for a given phased array, increasing $|l|$ widens the beam. Therefore, to have both a narrow beam and large $|l|$ puts severe conditions on the array antenna. At the time of writing no radar system exists that can transmit the required beams to detect the OAM associated with the considered large scale plasma flows. On the other hand, it may be noted that whereas we have only considered plasma flows of the order of the radar beam diameter or larger it may very well be that smaller scale plasma vortices exist which many together filling a major part of the beam cross section could be detected by a radar. In this case it seems possible that higher frequency shifts due to the OAM could be detected, since smaller vortices may exhibit higher rotational frequencies.

[44] The discussion of the detection of rotational plasma flows above involved the scatter of a transmitted twisted beam off the plasma flow. OAM need not be measured in the detected radiation in this case. The situation is different with coherent scatter off beams of electrostatic plasma waves that carry OAM. To detect such beams the involved transmitted and received radar beams, together with the plasma beam, must fulfill a matching condition on the OAM mode number of the beams, in addition to the usual conditions on the frequencies and wave vectors. Further, in this case the scatter occurs at the Langmuir or ion acoustic frequency, instead of the small rotational frequency shift. However, whether plasma beams carrying OAM are naturally excited in the auroral plasma remains an open question.

[45] Several ways can be envisioned to detect OAM in the received scatter. When performing measurements it should be kept in mind that for a given phased array, changing the magnitude of l will also change the beam shape, which makes comparisons of detected scatter more difficult, for example, if one wished to compare the case $l \neq 0$ and $l = 0$ to discriminate between rotational and translational Doppler effects. OAM related effects in the scatter can instead be discriminated from those of statistically independent plasma fluctuations and Doppler broadening by comparing the scatter from two transmit–receive modes that have the same radar beam shape. By simply changing the sign of the azimuthal phase variation (l) in the beam we change the sign of OAM without changing the beam shape. For example, the results for transmitting a beam with $l = +1$ and receiving with the same $l = +1$ can be compared to the results for transmitting $l = +1$ and receiving with a beam having the opposite twist $l = -1$. Scatter from statistically independent fluctuations is independent of the antenna phasing. On the other hand, if the scattering medium has imparted OAM on the scattered field there would be an asymmetry with respect to the sign of l in the detected scatter. In the same way effects of non-Maxwellian distributions and plasma flows not strictly transverse to the geomagnetic field that are not associated with OAM can be distinguished. Any frequency shift that does not depend on the phasing l can be attributed to Doppler shift due to plasma motion along the beam axis. In the present treatment we have studied limited geometries to illustrate the essential mechanisms involved. These geometries, if occurring, may only approximately hold for too short periods of time since geophysical conditions can change during a radar integration period. However, OAM related effects can nevertheless be detected by comparing the scatter for opposite signs of the phasing l.

[46] Finally, not only twisted beams are sensitive to plasma flows transverse to the beams. The beam divergence of regular beams is associated with wave vector components transverse to beam axis, which interact with the transverse plasma flows and thus give a Doppler broadening of the backscattered signal. For the auroral ionosphere this Doppler broadening is generally larger than the rotational frequency shift due to the OAM content of the beam for the cases considered in the present treatment.

[47] The width of the ion line spectrum influences estimates of the ion temperature. If the measured spectral width is attributed solely to temperature effects or if Doppler broadening is taken into account will give a different temperature. It seems that the overestimation of temperatures

would not be large enough to significantly affect previous statistical studies of Joule heating. However, the spectral broadening due to transverse plasma motion and beam divergence could be important for relatively rare events with very high flow velocities and at incoherent scatter facilities with large beam divergence.

[48] **Acknowledgments.** The authors gratefully acknowledge Craig Heinselman and Yakov Istomin for discussions, as well as the reviewers for constructive comments.

References

Allen, L., M. W. Beijersbergen, R. J. C. Spreeuw, and J. P. Woerdman (1992), Orbital angular momentum of light and the transformation of Laguerre-Gaussian laser modes, *Phys. Rev. A*, *45*(11), 8185–8189, doi:10.1103/PhysRevA.45.8185.

Borovsky, J. E., D. M. Suszcynsky, M. I. Buchwald, and H. V. DeHaven (1991), Measuring the thicknesses of auroral curtains, *Arctic*, *44*(3), 231–238.

Cosgrove, R. B., and M. Codrescu (2009), Electric field variability and model uncertainty: A classification of source terms in estimating the squared electric field from an electric field model, *J. Geophys. Res.*, *114*, A06301, doi:10.1029/2008JA013929.

Courtial, J., D. A. Robertson, K. Dholakia, L. Allen, and M. J. Padgett (1998), Rotational frequency shift of a light beam, *Phys. Rev. Lett.*, *81*(22), 4828–4830, doi:10.1103/PhysRevLett.81.4828.

Fried, B. D., and S. D. Conte (1961), *The Plasma Dispersion Function*, Academic, New York.

Garetz, B. A. (1981), Angular doppler effect, *J. Opt. Soc. Am.*, *71*(5), 609–611, doi:10.1364/JOSA.71.000609.

Gori, F., M. Santarsiero, R. Borghi, and G. Guattari (1998), Orbital angular momentum of light: a simple view, *Eur. J. Phys.*, *19*, 439–444, doi:10.1088/0143-0807/19/5/005.

Haerendel, G., B. U. Olipitz, S. Buchert, O. H. Bauer, E. Rieger, and C. L. Hoz (1996), Optical and radar observations of auroral arcs with emphasis on small-scale structures, *J. Atmos. Terr. Phys.*, *58*, 71–83, 1996.

Hagfors, T. (1961), Density fluctuations in a plasma in a magnetic field, with applications to the ionosphere, *J. Geophys. Res.*, *66*, 1699–1712, doi:10.1029/JZ066i006p01699.

Istomin, Y. N. (2002), The ponderomotive action of a powerful electromagnetic wave on ionospheric plasma, *Phys. Lett. A*, *299*, 248–257.

Jackson, J. D. (1999), *Classical Electrodynamics*, John Wiley, New York.

Knudsen, D., G. Haerendel, S. Buchert, M. Kelley, Å. Steen, and U. Brändström (1993), Incoherent scatter radar spectrum distortions from intense auroral turbulence, *J. Geophys. Res.*, *98*, 9459–9471.

Knudsen, H. L. (1953), The field radiated by a ring quasi-array of an infinite number of tangential or radial dipoles, *Proc. IRE*, *41*(6), 781–789, doi:10.1109/JRPROC.1953.274261.

Lanchester, B. S., M. H. Rees, K. J. F. Sedgemore, J. R. Palmer, H. U. Frey, and K. U. Kaila (1998), Ionospheric response to variable electric fields in small-scale auroral structures, *Ann. Geophys.*, *16*, 1343–1354, doi:10.1007/s00585-998-1343-81998.

Leyser, T. B., L. Norin, M. McCarrick, T. R. Pedersen, and B. Gustavsson (2009), Radio pumping of ionospheric plasma with orbital angular momentum, *Phys. Rev. Lett.*, *102*(6), 065004, doi:10.1103/PhysRevLett.102.065004.

Maggs, J. E., and T. N. Davis (1968), Measurements of the thicknesses of auroral structures, *Plant. Space Sci.*, *16*(2), 205–209, doi:10.1016/0032-0633(68)90069-X.

Mendonça, J. T., S. Ali, and B. Thidé (2009a), Plasmons with orbital angular momentum, *Phys. Plasmas*, *16*(11), 112103, doi:10.1063/1.3261802.

Mendonça, J. T., B. Thidé, and H. Then (2009b), Stimulated Raman and Brillouin backscattering of collimated beams carrying orbital angular momentum, *Phys. Rev. Lett.*, *102*(18), 185005, doi:10.1103/PhysRevLett.102.185005.

Mohammadi, S. M., L. K. S. Daldorff, J. E. S. Bergman, R. L. Karlsson, B. Thidé, K. Forozesh, T. D. Carozzi, and B. Isham (2010a), Orbital angular momentum in radio — a system study, *IEEE Trans. Ant. Prop.*, *58*(2), 565–572, doi:10.1109/TAP.2009.2037701.

Mohammadi, S. M., L. K. S. Daldorff, K. Forozesh, B. Thidé, J. E. S. Bergman, B. Isham, R. Karlsson, and T. D. Carozzi (2010b), Orbital angular momentum in radio: Measurement methods, *Radio Sci.*, *45*, RS4007, doi:10.1029/2009RS004299.

Molina-Terriza, G., J. P. Torres, and L. Torner (2007), Twisted photons, *Nat. Phys.*, *3*, 305–310, doi:10.1038/nphys607.

Sandahl, I., T. Sergienko, and U. Brändström (2008), Fine structure of optical aurora, *J. Atmos. Sol.-Terr. Phys.*, *70*(18), 2275–2292, doi:10.1016/j.jastp.2008.08.016.

Swartz, W. E. (1978), Analytic partial derivatives for least-squares fitting incoherent scatter data, *Radio Sci.*, *13*, 581–589.

Thidé, B., H. Then, J. Sjöholm, K. Palmer, J. Bergman, T. D. Carozzi, Y. N. Istomin, N. H. Ibragimov, and R. Khamitova (2007), Utilization of photon orbital angular momentum in the low-frequency radio domain, *Phys. Rev. Lett.*, *99*(8), 087701, doi:10.1103/PhysRevLett.99.087701.

Weideman, J. A. C. (1994), Computation of the complex error function, *SIAM J. Num. Anal.*, *31*(5), 1497–1518.